

Unique morphology of Interhemispheric Field-aligned Currents and the Associated Factors and Mechanism

Pengyu Zhang¹, Yang-Yi Sun¹, Chieh-Hung Chen²

¹China university of Geosciences (Wuhan), China (zhangpengyu@cug.edu.cn);

²Chengdu University of Technology, China (nononochchen@gmail.com);

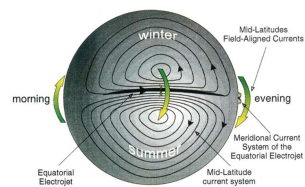


EGU25-6423



1. Introduction

The ionosphere owns a complex electric current system mainly driven by the ionospheric electric field and thermospheric wind. The most significant feature of the ionospheric current is the **Solar quiet (Sq) current** which is consist of two vortices currents in the northern and southern hemispheres. The **Interhemispheric Field-aligned currents (IHFACs)** alongside the geomagnetic lines like a bridge connecting the two vortices that promote the balance of north-south current system (Figure 1).



Recent studies found that ionospheric current exhibit complex variations that far beyond the original thoughts (Zhang et al., 2023, 2024). This study analysis different factors of ionospheric dynamo to explore the cause of the unique characteristic of the regional ionospheric current variations.

Figure 1. The diagram of the IHFACs (Olsen, 1997).

2. Data and Methodology

This study utilize the ground-based and space-borne geomagnetic data and thermospheric wind data measured by TIMED/TIDI. The equivalent current method was used to calculate the horizontal Sq current (Yamazaki and Maute, 2017) and the **two-step method** was developed to determine the Sq focus (Zhang et al., 2023). The ionospheric radial currents (IRCs) derived by satellite magnetic data which are published at European Space Agency. IRCs are contributed by both IHFACs and F-region current. The IHFACs can derived from IRCs by the function,

$$IHFACs = B_F \cdot \frac{IRC_N \cdot \cos(I_S) - IRC_S \cdot \cos(I_N)}{\sin(I_N) \cdot B_{F,N} - \sin(I_S) \cdot B_{F,S}}$$

where IRC_N and IRC_S are the IRC at the two conjugate points of the same geomagnetic line in northern and southern hemispheres, I_N and I_S are the geomagnetic inclinations, B_F is the geomagnetic intensity. The ionospheric conductivities are derived from the IRI-2020 and Nrlmsise-00 models according to the empirical ionospheric conductivity formulas (Schunk & Nagy, 2009).

3. Variations of Sq Current Over East Asia

Two-step method (Zhang et al., 2023) can help us to determine the Sq focus (Center of Sq current vortex) and track the trajectory. The result suggest the Sq focus move from southeast to northwest over East Asia and the morphology of Sq are gradually deformed into a tilted ellipse (Figure 2).

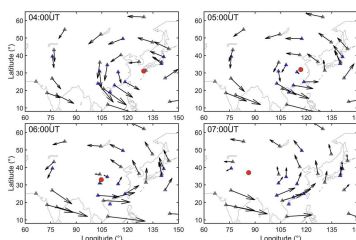


Figure 2. Trajectory of Sq focus over East Asia from 04:00 to 07:00 UT in winter (Zhang et al., 2023).

where W_p is the non-migrating wind vary with longitude (λ), B is the vertical geomagnetic field, s is the wavenumber, R is the wind amplitude, and k is the wave order. The polarized current (J_{Ep}) can be estimated by the formula:

$$J_{Ep} = \sum \vec{\sigma} \cdot (-W \times B)$$

We further overlay J_{Ep} onto Sq to estimate the impact on the trajectory and morphology. The results suggest that the **polarization** generated by the **regional winds** are the cause of the **northwestward shift** of Sq focus and **tilted deformation**.

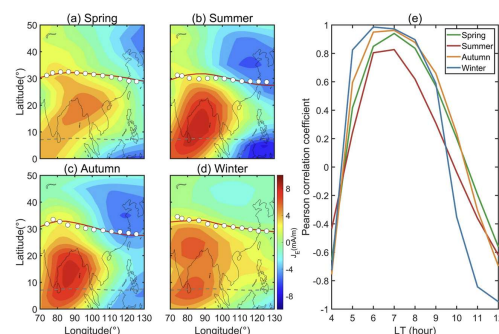


Figure 4. comparison of the determined (white points) and estimated (red lines) trajectory (Zhang et al., 2024).

The thermospheric winds vary in different regions can cause regional polarization in ionosphere (Kil et al., 2007; Zhang et al., 2024). The sketch are shown in Figure 3. This study derive the equation to estimate the polarized electric field (E_p),

$$E_p = \int |W_p(\lambda) \times B| d\lambda$$

$$= \int_{k=0.5/s}^{k+0.5/s} |R_{\Omega}^2 \cos(2\pi s\lambda + \varphi) \cdot B| d\lambda = \frac{4}{\pi} R_{\Omega}^2 \cdot B$$

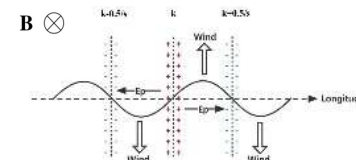


Figure 3. Sketch of non-migrating tides generate regional polarization in ionosphere (Zhang et al., 2024).

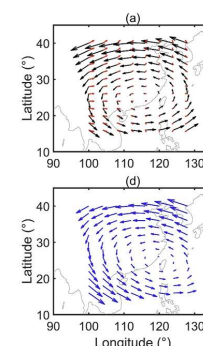


Figure 5. Simulation of Sq current deformation (Zhang et al., 2024).

4. Reversal of IHFACs

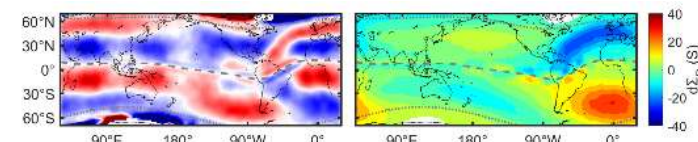


Figure 6. Global distribution of IHFACs (left panel) and Pedersen conductivity difference between South and North Hemisphere (right panel). Red and blue in left panel represent the IRCs flow out and into the ionosphere.

The “C”-shaped reversal over the American-Atlantic region is remarkable. Previous studies speculated that the “C”-shaped reversal may be influenced by conductivity, wind, or particle precipitation (Park et al., 2020; Wang et al., 2023; Archana & Arora, 2024). Our results suggest that the **hemispheric asymmetry of Pedersen conductance**, $d\Sigma_p$, display a significant “C”-shaped morphology, is the cause for the **reversal of IHFACs**.

The “two-seasons” climate features of low-latitude IHFACs, resembling the behavior of the non-migrating tides (Oberheide et al., 2011), suggest that these tides can modulate the low-latitude IHFACs. The wavenumber of low-latitude IHFACs (4 or 5) is one more than that of the thermospheric winds (3 or 4), which is attributed to the truncation of the “C”-shaped reversal over South America.

5. Conclusion

Both the non-migrating thermospheric wind and ionospheric conductance can significantly modulate the regional ionospheric variations. The regional wind can deform and shift the Solar quiet current. The global tides can force the Interhemispheric Field-Aligned Current show significant longitudinal variations. The asymmetry of Pedersen conductance between South and North Hemisphere can reverse the IHFAC directions.

Acknowledgments:

The authors acknowledge the Geomagnetic Network Center of China and INTERMAGNET for providing geomagnetic data. The authors acknowledge European Space Agency for providing IRCs data. The authors acknowledge High Altitude Observatory for providing the lower thermospheric wind data.

References:

- Oberheide et al. (2011). <https://doi.org/10.1029/2010JA015911>
- Olsen, N. (1997). <https://doi.org/10.1029/96JA02949>
- Schunk & Nagy (2009). Ionospheres: Physics, Plasma Physics, and Chemistry. Yamazaki, Y., & Maute, A. (2017). <https://doi.org/10.1007/s11214-016-0282-z>
- Zhang et al. (2023). <https://doi.org/10.1029/2022EA002572>
- Zhang et al. (2024). <https://doi.org/10.1029/2023JA032381>